

UC Davis

UC Davis Previously Published Works

Title

Inhibition of myeloperoxidase: Evaluation of 2H-indazoles and 1H-indazolones

Permalink

<https://escholarship.org/uc/item/52m0x3g5>

Journal

Bioorganic & Medicinal Chemistry, 22(22)

ISSN

0968-0896

Authors

Roth, Aaron
Ott, Sean
Farber, Kelli M
et al.

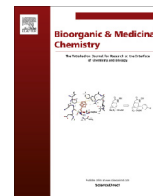
Publication Date

2014-11-01

DOI

10.1016/j.bmc.2014.09.044

Peer reviewed



Inhibition of myeloperoxidase: Evaluation of 2H-indazoles and 1H-indazolones



Aaron Roth^a, Sean Ott^b, Kelli M. Farber^a, Teresa A. Palazzo^a, Wayne E. Conrad^a, Makhlu J. Haddadin^c, Dean J. Tantillo^a, Carroll E. Cross^b, Jason P. Eiserich^b, Mark J. Kurth^{a,*}

^a Department of Chemistry, University of California, One Shields Avenue, Davis, CA 95616, United States

^b Department of Internal Medicine, Division of Pulmonary/Critical Care Medicine, 4150 V Street, Suite 3100, Sacramento, CA 95817, United States

^c Department of Chemistry, American University of Beirut, Beirut, Lebanon

ARTICLE INFO

Article history:

Received 17 July 2014

Revised 13 September 2014

Accepted 20 September 2014

Available online 2 October 2014

Keywords:

Myeloperoxidase

Davis–Beirut reaction

2H-Indazole

Structure–activity relationship

Computational docking

ABSTRACT

Myeloperoxidase (MPO) produces hypohalous acids as a key component of the innate immune response; however, release of these acids extracellularly results in inflammatory cell and tissue damage. The two-step, one-pot Davis–Beirut reaction was used to synthesize a library of 2H-indazoles and 1H-indazolones as putative inhibitors of MPO. A structure–activity relationship study was undertaken wherein compounds were evaluated utilizing taurine-chloramine and MPO-mediated H₂O₂ consumption assays. Docking studies as well as toxicophore and Lipinski analyses were performed. Fourteen compounds were found to be potent inhibitors with IC₅₀ values <1 μM, suggesting these compounds could be considered as potential modulators of pro-oxidative tissue injury perturbed by the inflammatory MPO/H₂O₂/HOCl/HOBr system.

© 2014 Elsevier Ltd. All rights reserved.

1. Introduction

Myeloperoxidase (MPO), primarily found in azurophilic granules of polymorphonuclear neutrophils (PMNs), is a key component of the innate immune response.^{1–5} Specifically, MPO acts as an important antimicrobial effector through its enzymatic production of hypohalous acids (e.g., HOCl, HOBr). These acids promote phagosomal oxidative antimicrobial activities, but if secreted or released extracellularly, can present a potent instigator of cell and tissue damage in the inflammatory milieu.² Active MPO has been found in or associated with a variety of disorders including atherosclerosis, Alzheimer's disease, neutrophil mediated glomerular injury, and idiopathic pulmonary fibrosis.²

Mediation of the effects of MPO related oxidative stress in patients with cystic fibrosis is a particularly pressing challenge. Cystic fibrosis (CF) is an autosomal recessive disease caused by mutations in a single gene encoding the glycoprotein CF transmembrane conductance regulator (CFTR). Loss of CFTR function in respiratory tract (RT) tissues results in a thickened, underhydrated RT mucus secretion. This in turn leads to reduced mucociliary airway clearance, airway bacterial colonization, infection, and an overly exuberant dysregulated RT inflammatory response

characterized by an intense airway neutrophil influx.⁶ Overactive recruited neutrophil effector proteolytic and oxidative processes are believed to represent the most debilitating feature of CF leading to progressively more severe RT disease and eventual RT failure, which characterizes end stage CF.^{6,7}

Neutrophil-derived MPO, known to represent the strongest and most abundant oxidative effector system in neutrophils, is present in CF RT fluids in early stages of the disease⁸ and in increasingly large quantities in later stages of the disease.⁹ Indeed, both circulating and RT MPO levels have been found to correlate with disease severity in CF.^{7,10,11} MPO's extracellular releases are suspected to play an important role in the pathophysiology of numerous other inflammatory diseases including both RT and cardiovascular diseases through its (i) direct oxidation and (ii) production of hypohalous acids.^{5,12–16}

In CF patients with advanced RT disease, opportunities exist for the development of small molecules to target the major molecular components of the neutrophil proteolytic and oxidative related mediators of RT pathobiology.¹³ One such pathway is represented by MPO. In addition to its high concentration in the RT of CF patients,^{9,14} there is evidence that MPO polymorphisms which lead to greater levels of MPO and mRNA and protein expressions are associated with more severe CF lung disease.¹⁷ Thus, MPO has been recognized as a viable drug target,¹⁸ a concept strengthened by the finding that inhibition of

* Corresponding author. Tel.: +1 530 554 2145; fax: +1 530 752 8995.

E-mail address: mjkurth@ucdavis.edu (M.J. Kurth).

MPO ameliorates an animal model of chronic RT inflammatory disease,¹⁹ we know of no studies to date that have directly addressed the effects of inhibition or absence of MPO in CF RT pathobiology. This is the case even though several promising recent experimental approaches have been designed to therapeutically target pro-oxidative MPO activities.^{20,21}

The structural similarity of 2*H*-indazoles to previously reported MPO inhibitors, such as indoles and hydroxamic acids, inspired our exploration of their inhibitory activity. Furthermore, we hypothesized that 2*H*-indazoles and 1*H*-indazolones would have greater bioavailability due to the second polar nitrogen in the core scaffold. Specifically, we sought to examine chain length tolerance at the synthetically accessible N¹, N², and C³ positions as well as the effect of polar, non-polar and aromatic substituents. Since terminal polar substituents on long alkyl chains have been shown to be a beneficial structural motif in previous MPO inhibitors,²² a subset of this initial library containing this feature was synthesized in hopes of replicating these previous successes. Herein, we describe the synthesis, computational analysis, structure–activity relationship (SAR) insights, and evaluation of 2*H*-indazoles and 1*H*-indazolones as inhibitors of MPO.

2. Results and discussion

2.1. Chemistry

The 3-alkoxy-2*H*-indazoles employed in this study were prepared by the versatile Davis–Beirut reaction (DBR)^{23–29} on 2-nitrobenzylamine **3**, in turn prepared by one of two complementary methods: (i) commercially available 2-nitrobenzyl bromide (**1**) was used to *N*-alkylate the requisite amine to form intermediate **3** (Scheme 1/Method A) or (ii) **3** was prepared by reductive amination of the requisite 2-nitrobenzaldehyde (Scheme 1/Method B). Regardless of the route to **3**, this 2-nitrobenzylamine intermediate need not be isolated. Rather, the DBR is initiated by direct addition of alcoholic potassium hydroxide to the Method A or Method B reaction mixture containing **3**, which leads to the targeted 3-alkoxy-2*H*-indazole **4** in good to excellent overall yield (49–87% for this two-step, one-pot process).

Likewise, the 1*H*-indazolones (**5** and **6**; Scheme 1) employed in this study were prepared through one of two complementary

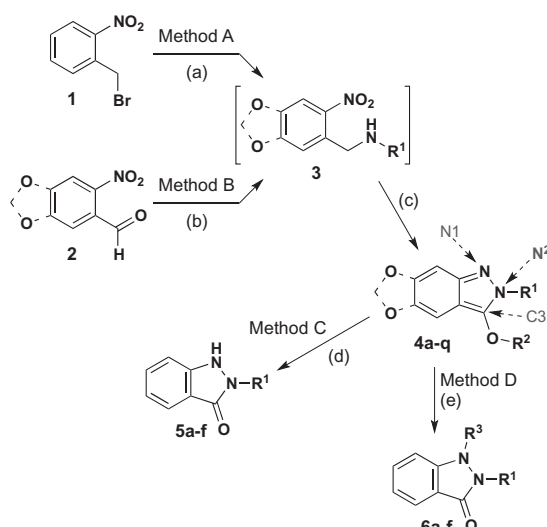
methods from the DBR-derived 3-alkoxy-2*H*-indazole **4**. In the first method (C), 3-alkoxy-2*H*-indazole **4** was heated to 100 °C in 0.3 M methanolic H₂SO₄ to affect a proto-dealkylation (e.g., loss of R²) reaction to deliver the targeted N¹-unsubstituted 1*H*-indazolone **5** (52–94% yield). In the second method (D), N¹-substituted 1*H*-indazolone **6** was obtained by an electrophile-mediated domino N¹-alkylation/O-dealkylation process, which provides the targeted heterocycle in excellent yield (70–95%).

Finally, the R¹-constrained 2*H*-indazole analogs—that is, containing N²–C³ fused ring systems—employed in this study (see **9** ⇒ **7** and **12** ⇒ **11**; Scheme 2) were obtained by intramolecular nucleophilic attack onto the corresponding DBR nitroso-imine intermediate (cf., **8** → **9**). Conventionally, hydroxyl has been the internal nucleophile utilized in R¹-constrained DBRs, which provides access to oxazolino- (**9**; *n* = 1) and oxazino-2*H*-indazoles (**9**; *n* = 2; Scheme 2). However, recent advances have expanded the scope of the R¹-constrained DBR to include thiol as the internal nucleophile.³⁰ In this modification, *N*-(2-nitrobenzyl)-2-(tritylthio)alkylamine **10**, formed from **2** via Method B, is trityl deprotected with TFA to give thiol **11**, which is then subjected to R¹-constrained DBR conditions to deliver the thiazolino- (**12a,b**; *n* = 1) and thiazino-2*H*-indazoles (**12b,c**; *n* = 2) in 66–83% yield.

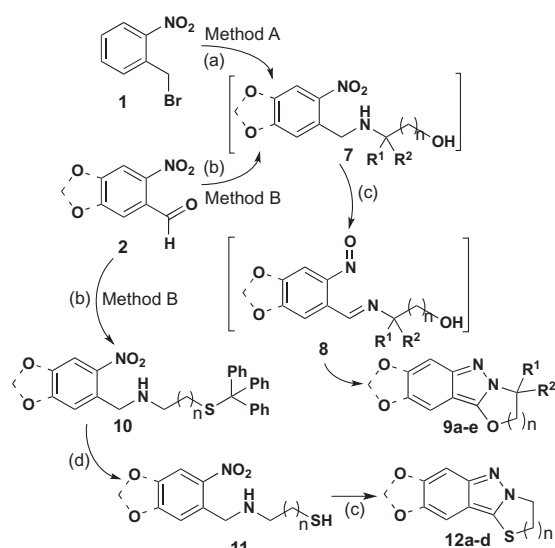
2.2. Molecular docking

Computational docking, performed using FRED (OpenEye software suite),^{31–33} was utilized to help characterize interactions within the active site. Docking study validation was accomplished through comparative docking of the 5-fluoroindole scaffold described by Soubhye,²² and HX1²⁰ bound in the active site of MPO [Fig. 1; (PDB ID 4C1M), RMSD docked vs natural is 1.2 Å]. Also included in the docking studies was 4-aminobenzoic acid hydrazide, the internal control for the assays discussed herein, which consistently displayed an IC₅₀ of 81 ± 19 nM.

These docking studies indicated that the 2*H*-indazoles, like previously reported inhibitors, likely sit in a stacked fashion over the heme lending credence to our inhibitor design approach. For example, compound **4a** (Fig. 2) is positioned in such a way that the alkyl chain on the N²-position extends out toward the hydrophobic pocket, while the aromatic core scaffold stacks over the pyrrole rings of the heme porphyrin.



Scheme 1. Reagents and conditions: (a) H₂NR¹, DIPEA, R²OH (solvent); (b) H₂NR¹, AcOH, R²OH (solvent) then NaCNBH₃; (c) KOH in 10% H₂O (v/v), 65 °C; (d) 0.3 M methanolic H₂SO₄/sealed vial, 100 °C; and (e) R³X, CH₃CN, reflux.



Scheme 2. Reagents and conditions: (a) H₂N(CH₂)_nOH, DIPEA, *i*PrOH; (b) H₂N(CH₂)_nOH (→ **9**) or H₂N(CH₂)_nSTr (→ **10**), DIPEA, *i*PrOH; then NaCNBH₃; (c) KOH in 10% H₂O (v/v), 65 °C; and (d) TFA, TES, DCM, 1 h, rt.

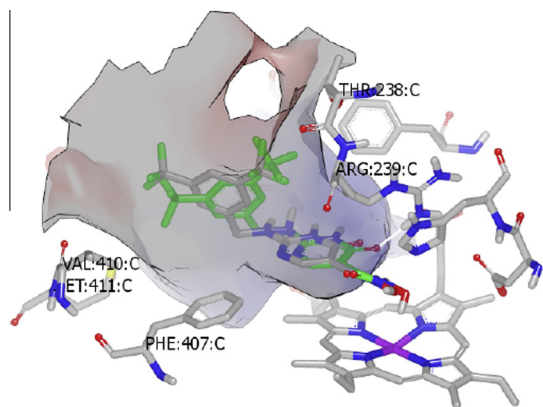


Figure 1. Structural layover of naturally bound HX1 (green) and docked HX1 (grey) indicating an effective docking model (RMSD = 1.2 Å).

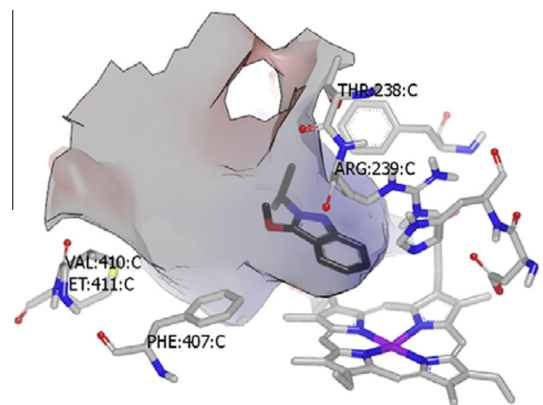


Figure 2. Compound **4a** docked into the active site of MPO (crystal structure obtained from PDB ID 4C1M).

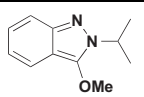
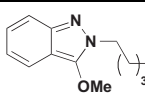
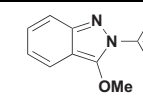
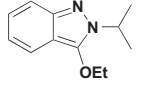
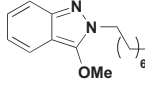
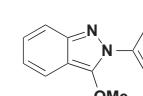
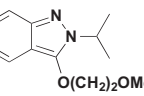
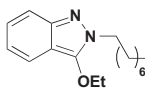
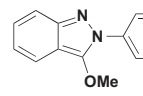
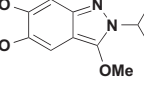
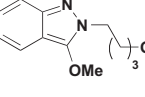
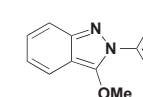
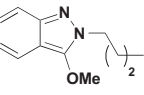
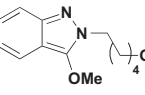
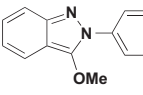
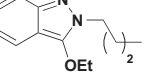
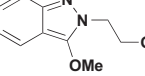
2.3. Structure–activity relationship

4-Aminobenzoic acid hydrazide was used as an internal control while MPO inhibitory activity was assessed using a taurine-chloramine assay to measure enzymatic hypochlorous acid production. Select IC_{50} values were confirmed utilizing a H_2O_2 -specific electrode allowing for real time hydrogen peroxide concentration measurements (Supporting information). Upon generation of an initial library of 2*H*-indazoles (Table 1), a consistent trend was found wherein, as the length of the chain increased, there was a dramatic decrease in inhibitory potency. For example, increasing the length of the chain from four (**4f**) to five (**4g**) carbons resulted in a three-fold decrease in potency. Compound **4l** was included to ensure that this decrease in efficacy was not a result of reduced solubility. The compounds synthesized containing terminal polar substituents (**4j–4l**, Table 1) failed to elicit a significant increase in inhibitory activity. It is possible that these modifications were not effective due to a change in orientation of the inhibitor with respect to the indole scaffold or because the alcohol moiety failed to carry a positive charge necessary to lower binding energy. A series of *N*²-aryl analogs (**4m–4q**) was included to explore the effects of more rigid, hydrophobic substituents that likely extend into the pocket of the MPO active site, but these compounds failed to produce an appreciable increase in inhibitor activity.

Lastly, by lengthening the alkoxy substituent at C³, we also sought to probe the relationship between substituents on the 3-position of both scaffolds [e.g.; **4a** –OMe → **4b** –OEt → **4c** –O(CH₂)₂OMe]. With this SAR study, we noted decreased inhibition of MPO as the length of the alkoxy chain was extended past two carbons. This trend is likely the result of increased inhibitor size within the relatively small distal portion of the active site.

As before, docking studies of the synthesized inhibitors indicate that the aromatic portion of the inhibitors is positioned in a π -stacking fashion over pyrrole ring D of the heme, while the hydrophobic portion extends into the cavernous hydrophobic pocket. If hydrogen bond donors are present, they are generally oriented toward the carboxylate groups of the heme. Because the

Table 1
 IC_{50} values of 3-alkoxy-2*H*-indazoles assessed with a taurine chlorination assay (154 mM NaCl, 30 μ M H_2O_2 , and 2 nM MPO)

Compound	IC_{50} (nM)	Compound	IC_{50} (nM)	Compound	IC_{50} (nM)
	704 ± 243		3876 ± 2550		2029 ± 1542
	722 ± 123		>10,000		4771 ± 2811
	1404 ± 105		>10,000		2000 ± 615
	711 ± 300		1787 ± 1221		1660 ± 1391
	910 ± 530		1539 ± 476		1102 ± 318
	807 ± 402		1078 ± 227		

All IC_{50} values are expressed in nM as a mean of ≥ 3 trials \pm standard deviation.

same orientation was maintained, it followed that increasing steric bulk at the C³-position would decrease inhibitor activity due to the constraints of the active site. Interestingly, docking studies indicated that incorporation of the benzodioxole ring (**4a** → **4d**) changes the inhibitor orientation in the active site. Here, rather than the aromatic core of the inhibitor occupying the space directly above the iron, the inhibitor is shifted such that the benzodioxole ring is positioned above the heme iron center (Fig. 3).

Owing to the presence of a basic nitrogen in the core scaffold and mildly acidic assay conditions, a portion of the inhibitor is expected to exist in the protonated form. Therefore, a protonated form of each molecule was docked for comparison. It was found that, in some cases, protonation created the opportunity for additional hydrogen bond and charge–charge interactions with the carboxylate groups of the heme. It should be noted that, in this instance, a direct correlation between IC₅₀ values and docking scores was not obtained, as is often the case with conventional docking programs.³⁴

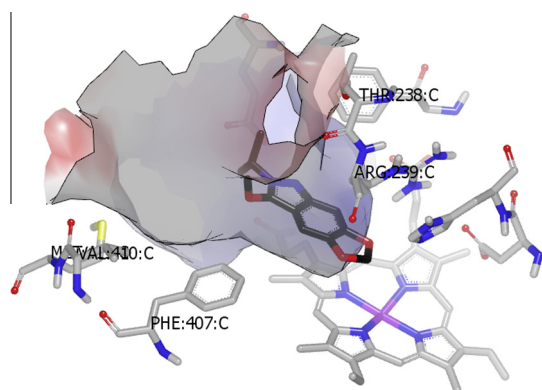


Figure 3. Compound **4d** in the MPO active site. The benzodioxole moiety now resides over the heme center while the tethered ring extends into the hydrophobic pocket.

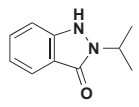
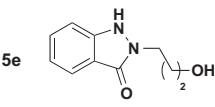
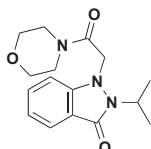
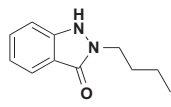
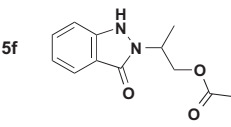
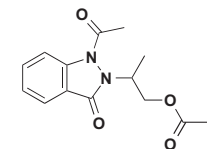
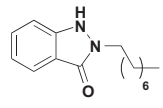
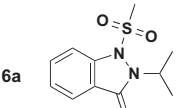
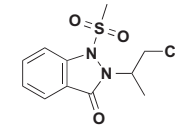
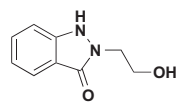
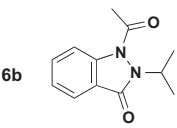
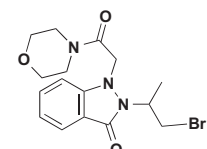
Interestingly, conversion of 3-alkoxy-2*H*-indazoles to the corresponding N¹-substituted 1*H*-indazolones resulted in significantly decreased inhibitory activity while the unsubstituted 1*H*-indazolones retained inhibitory potency (Table 2). Docking studies indicate that if N¹-substituted 1*H*-indazolones were to enter the active site, they would likely adopt a pose similar to the N¹-unsubstituted 1*H*-indazolones. We hypothesize that substituents at the N¹-position result in the loss of a crucial interaction with either the carboxylate groups of the heme or the glutamate anion within the active site.³⁵ These observations are consistent with the findings of Sliskovic³⁵ wherein N-alkylation of the indole scaffold resulted in reduced inhibitor potency. Based on these SAR results, it is clear that either the accessible lone pair or nucleophilic nitrogen is essential for inhibitory activity.³⁵

When studying the 5-fluoroindole scaffold, Soubhye²² found that compounds with longer alkyl chains in the 3-position displayed better inhibitory efficacy than their ‘less greasy’ counterparts. In the case of these indazolo analogs, it is interesting to note that increasing the length of the alkyl chain of N² or C³ was only beneficial to a certain point. For example, a branched alkyl chain (isopropyl; **4a**) was well tolerated, while an *n*-pentyl (**4g**) or *n*-octyl chain (**4h**) decreased inhibitory activity. It is important to note that increasing the length of an alkyl chain can cause issues with solubility or with the molecule’s ability to enter the active site, even if it may be beneficial within the active site.

We next set out to explore the use of constrained analogs of the 2*H*-indazole scaffold—that is, containing N²–C³ fused ring systems—in hopes that this would facilitate passage through the narrow pore to the exposed heme. A series of both substituted and unsubstituted oxazolino- and oxazinoindazoles were synthesized. Also, taking advantage of newly developed methodology to access substituted and unsubstituted thiazolino- and thiazino-2*H*-indazoles,³⁰ we were able to explore variation of the heteroatom substituent at the C³-position. Indeed, it was found that both ring size and the nature of the heteroatom are determining factors in inhibitory potency. Constraining the N²-position resulted in significantly increased inhibitory activity by possibly facilitating

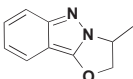
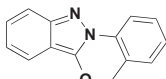
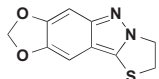
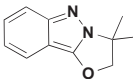
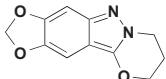
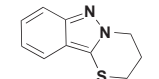
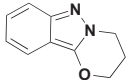
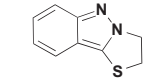
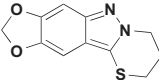
Table 2

IC₅₀ values of 1*H*-indazolones assessed with a taurine chlorination assay (154 mM NaCl, 30 μM H₂O₂, and 2 nM MPO)

Compound	IC ₅₀ (nM)	Compound	IC ₅₀ (nM)	Compound	IC ₅₀ (nM)
	660 ± 222		1948 ± 915		>10,000
	792 ± 380		2121 ± 1474		>10,000
	>10,000		>10,000		>10,000
	2469 ± 1251		>10,000		>10,000

All IC₅₀ values are expressed in nM as a mean of ≥3 trials ± standard deviation.

Table 3
IC₅₀ values of constrained 2*H*-indazole analogs assessed with a taurine chlorination assay (154 mM NaCl, 30 μM H₂O₂, and 2 nM MPO)

Compound	IC ₅₀ (nM)	Compound	IC ₅₀ (nM)	Compound	IC ₅₀ (nM)
9a 	900 ± 466	9d 	4148 ± 128	12b 	87 ± 7
9b 	1028 ± 427	9e 	403 ± 128	12c 	213 ± 22
9c 	359 ± 89	12a 	94 ± 18	12d 	140 ± 33

All IC₅₀ values are expressed in nM as a mean of ≥ 3 trials ± standard deviation.

entrance into the active site (Table 3). Furthermore, by changing from an oxygen substituent (9c) to a sulfur substituent (12c) in the tethering ring, a 40% improvement in potency was observed. Additional improvement (56%) was observed when the tethering ring size was reduced from six- (12c) to five-membered [12a; note that the *O*-analog of 12a (i.e., 'S' replaced with 'O'), unlike substituted versions 9a and 9b, is unstable²³]. Seeking to build upon these successes, we set out to incorporate the benzodioxole moiety into the *S*-constrained scaffold (i.e., 12a → 12b), which docking studies suggest causes a change in the orientation of the inhibitor in the active site (see Supporting information/12b/p. S25). To our delight, incorporation of the 1,3-benzodioxole ring provided markedly improved inhibitory activity (see 12b and 12d; Table 3) and we speculate that addition of the benzodioxole ring reduces the likelihood of electrophilic attack and/or MPO compound I mediated oxidation.³⁶ To confirm that the observed active inhibitors 12a–d are the unoxidized thiazino- or thiazolino-systems, rather than the corresponding sulfoxides and/or sulfones, inhibitors 12a–d were treated with excess NaOCl and examined by liquid chromatography/mass spectrometry (LC/MS) at 1 h and 24 h. Only trace sulfoxide formation was detected at 24 h (detectable by MS, but not diode array).

Further computational analysis was undertaken to examine the drug-like properties for both classes of inhibitors using OpenEye software. As detailed in Table 4, the parameters examined included the presence of hydrogen bond donors (HBD) and hydrogen bond acceptors (HBA), Log*P*, 2D Polar Surface Area (PSA), and the potential for aggregation. It was found that, of the fourteen compounds which demonstrate potencies less than 1 μM, those containing less than two HBD and HBA's scored better with our docking methods. It is interesting to note that even with relatively few HBD and

HBA's, active 2*H*-indazoles and 1*H*-indazolones still maintain satisfactory calculated Log*P* values. For example, compound 12b was calculated to have a Log*P* of 1.72, while the protonated form of 4e, containing a comparatively greasy butyl substituent, has a calculated Log*P* of 3.94. In addition, Veber and Kopple found an increased probability of satisfactory oral bioavailability through passive diffusion existed if compounds contained a PSA of less than 140 Å² and fewer than ten rotatable bonds.³⁷ Additionally, Hou and Xu found that reduced polar surface area and molecular weight below 350 Daltons facilitates passage through the blood brain barrier.³⁸ Efficient passage through this barrier could prove essential in the treatment of diseases such as multiple sclerosis, Alzheimer's disease, and Parkinson's disease through inhibition of MPO.^{2,39} Furthermore, it was found that all 2*H*-indazoles and 1*H*-indazolones were unlikely to act as aggregators based on a structure based screen. This analysis underwrites the further consideration of the potential efficacy of these compounds as drugs. A complete tabulation of this analysis is available in Supporting information.

3. Conclusion

A series of 2*H*-indazoles and 1*H*-indazolones were synthesized utilizing the Davis–Beirut reaction, and evaluated as potential MPO inhibitors. Fourteen of these compounds displayed potent IC₅₀ values (nanomolar range) as assessed utilizing taurine-chloramine inhibition and H₂O₂ consumption assays. Compounds containing N¹-substituents were not effective inhibitors, while compounds with relatively small substituents at N² and C³ were most active. The most potent compounds in the series were constrained 2*H*-indazole analogs—that is, containing N²–C³ fused ring systems—with the most potent also incorporating a

Table 4
Drug like properties of select compounds (mean IC₅₀ values are shown)

Compound	HBD	HBA	XLog <i>P</i>	2D PSA	Molecular weight	Score	IC ₅₀ (nM)
12b	0	3	1.72	36.28	220.3	−44.74	87
12a	0	1	1.99	17.82	176.2	−46.65	94
12d	0	3	2.21	36.28	234.3	−41.23	140
12c	0	1	2.48	17.82	190.3	−43.61	213
9c	0	2	1.75	27.05	174.2	−38.09	359
9e	0	4	1.48	45.51	218.2	−35.45	403
5a	1	2	2.03	37.79	176.2	−39.94	660
4a	0	2	2.76	27.05	190.2	−47.20	704
4d	0	4	2.49	45.51	234.3	−63.55	711
4b	0	2	3.16	27.05	204.3	−50.03	722
5b	1	2	2.48	37.79	190.2	−48.13	792
4f	0	2	3.61	27.05	218.3	−53.95	807
9a	0	2	1.79	27.05	174.2	−39.72	900
4e	0	2	3.21	27.05	204.3	−50.64	910

See Supporting information for a complete tabulation of results.

1,3-benzodioxole ring. The present data suggests that, like the 2-thioxanthines,²¹ the recently described modified hydroxamates,²⁰ the tetramethyl and tetraethyl nitroxides⁴⁰ and targeted MPO-modulating oligopeptide,⁴¹ 2*H*-indazoles and 1*H*-indazolones should be considered for possible therapeutic inhibition of unwaranted MPO activity in inflammatory diseases characterized by episodes of heightened neutrophil activation and convincing evidences of MPO-related pro-oxidative tissue injury. Such investigations will need to take into consideration toxicology and pharmacokinetic activities in complex biological fluids such as plasma, joint fluids, respiratory tract mucus secretions, and in complex inflammatory milieu.

4. Experimental

4.1. Docking protocols

All docking was performed using the OpenEye Suite of programs.^{31–33} A receptor to model the MPO active site was set up using the Protein Data Bank (PDB) file 4C1M²⁰ utilizing the *FRED* receptor program. The series of molecules studied herein were built using *Gaussview 5.0.9* associated with *Gaussian09*⁴² and saved as a library (.oeb.gz). The 5-fluoroindole with inhibitory activity previously published by Soubhye²² was included in this library to ensure that our docking methods were sound. All small molecules in the library were subject to a conformational search using *Omega2*. The conformers of each small molecule were then docked into the active site using *FRED*. Chemgauss3 scoring was employed.

4.2. Taurine chlorination assay

Taurine chloramine was measured using a modified method from Dypbukt et al.⁴³ In a volume of 125 μ L, the final reaction mixture contained 6.8 mM taurine, 2 nM MPO, 105 mM NaCl, and various inhibitor concentrations in 20 mM phosphate buffer, pH 6.5. The reaction was initiated with 40 μ M H₂O₂, and after 5 min. was terminated with the addition of 4 μ g catalase. To determine the amount of taurine chloramine produced, an equal volume of color developing solution containing 500 μ M 3,3',5,5'-tetramethylbenzidine and 100 μ M sodium iodide in 300 mM acetate buffer, pH 5.4. Absorbance was measured in a spectrophotometric microplate reader (PowerWave; Biotek Instruments Inc.) at a wavelength of 650 nm.

4.3. H₂O₂ mediated MPO inhibition assay

H₂O₂ was measured using a H₂O₂-specific electrode (World Precision Instruments, Sarasota, FL). The electrode was submerged in a continuously stirred reaction vessel containing 30 μ M H₂O₂, 154 mM NaCl, and various inhibitor concentrations in 10 mM phosphate buffer, pH 7.4. The reaction was initiated with the addition of 10 nM MPO. Data was collected using a free radical analyzer (World Precision Instruments, Sarasota, FL) and a PowerLab data acquisition system (ADInstruments, Colorado Springs, CO).

4.4. Chemistry

All solvents and reagents were purchased from commercial suppliers and used without further purification. For reactions run in sealed microwave vials, oven-dried Biotage[®] 5–10 mL or 10–20 mL vials containing a Teflon-coated stirrer bar and sealed with a Teflon-lined septum were used. Analytical thin layer chromatography was carried out on pre-coated plates (Silica gel 60 F254, 250 μ m thickness) and visualized with UV light. Flash chromatography was performed with 60 Å, 35–70 μ m silica gel (Acros Organics). Concentration refers to rotary evaporation under reduced pressure.

¹H NMR spectra were recorded on Varian spectrometers operating at 600 MHz at ambient temperature with CDCl₃ or DMSO-*d*₆ as solvent. ¹³C NMR spectra were recorded on Varian spectrometers operating at 150 MHz at ambient temperature with CDCl₃ or DMSO-*d*₆ as solvent. Data for ¹H NMR are recorded as follows: chemical shift (δ , ppm), multiplicity (s, singlet; d, doublet; t, triplet; q, quartet; quint, quintet; m, multiplet; br, broad; app, apparent), integration, coupling constant (Hz). Chemical shifts are reported in parts per million relative to CDCl₃ (¹H, δ 7.26, ¹³C, δ 77.16), DMSO (¹H, δ 2.50, ¹³C, δ 39.5) or TMS (¹H, δ 0.00, ¹³C, δ 0.00). Infrared spectra were recorded on an ATI-FTIR spectrometer. The specifications of the LC/MS are as follows: electrospray (+) ionization, mass range 150–1500 Da, 20 V cone voltage, and Xterra MS C18 column (2.1 mm \times 50 mm \times 3.5 μ m).

4.4.1. General procedure for synthesis of 3-alkoxy-2*H*-indazoles—Method A (4a–4l)

2-Nitrobenzyl bromide (15.31 mmol) was dissolved in alcoholic solvent (typically MeOH or EtOH, 115 mL) and added dropwise to a stirring solution of requisite primary amine (61.2 mmol), DIPEA (61.2 mmol), and 38 mL of alcoholic solvent over 6 h and then left stirring overnight. Water (15 mL) and KOH (76.6 mmol) were then added and this mixture was heated at 60 °C for 24 h and monitored by thin layer chromatography. When the starting material had been consumed, 50 mL of water was added and the alcoholic solvent was removed under reduced pressure. This aqueous mixture was then extracted twice with dichloromethane. The combined organic extracts were washed with water and brine, dried over sodium sulfate, and concentrated. The crude mixture was purified by flash chromatography to afford the title compound.²³

4.4.2. General procedure for preparation of 3-alkoxy-2*H*-indazoles—Method B (4m–4p)

2-Nitrobenzaldehyde (5.22 mmol) and the requisite amine (6.26 mmol) were dissolved in alcoholic solvent (typically MeOH or EtOH, 13 mL) in a 250 mL round bottom flask. Glacial acetic acid (26.1 mmol) and sodium cyanoborohydride (6.26 mmol) were added and this solution was stirred at room temperature for 2.5 h. Additional alcoholic solvent (37 mL) and a solution of KOH (78.3 mmol) in water (6 mL) were added, a water-cooled reflux condenser was attached and this solution was heated at reflux for 2 h. The reaction mixture was then cooled to room temperature, water (20 mL) was added, and the alcoholic solvent was removed by rotary evaporation. This aqueous mixture was then neutralized with 1 N HCl and extracted with ethyl acetate (3 \times 30 mL). The combined organic extracts were then washed with 1 N HCl (40 mL), saturated sodium carbonate (40 mL), water (40 mL), and brine (40 mL), dried over anhydrous sodium sulfate, and concentrated and purified by flash chromatography to afford the title compound.²⁴

4.4.3. Synthesis of 2-(4-ethynylphenyl)-3-methoxy-2*H*-indazole (4q)

Compound **4o** (10.05 mmol) was added to a flame dried 250 mL round bottomed flask and dissolved in dry tetrahydrofuran (16 mL) under nitrogen gas. PdCl₂(PPh₃)₂ (0.50 mmol), CuI (1.00 mmol), and triethylamine (16 mL) were added and the reaction mixture cooled to 0 °C. Trimethylsilylacetylene (15.10 mmol) was added dropwise, then the reaction allowed to stir at room temperature. Formation of the protected silyl intermediate was complete after 1 h and 20 min as shown by TLC. Approximately 5 g of sodium carbonate was added to the reaction and allowed to stir for 12 h to effect removal of silyl protecting group. Water (10 mL) was added to the reaction and the reaction mixture was extracted with ethyl acetate (3 \times 30 mL). The organic extracts were combined, washed with brine, dried over anhydrous sodium sulfate, and purified by

flash chromatography (10% ethyl acetate/hexanes) to afford **4q** (1.952 g, 78% yield) as an off-white solid.

4.4.4. General procedures for the synthesis of substituted [1,3]oxazino[3,2-*b*]indazoles and 2,3-dihydrooxazolo[3,2-*b*]indazoles (9a–9d)

2-Nitrobenzyl bromide (15.31 mmol) was dissolved in THF (115 mL) and added dropwise to a stirring solution of requisite amino alcohol (61.2 mmol), DIPEA (61.2 mmol), and 38 mL of isopropanol over 6 h and then left stirring overnight. Water (15 mL) and KOH (76.6 mmol) were then added and this mixture was heated at 60 °C for 24 h and monitored by thin layer chromatography. When the starting material had been consumed, 50 mL of water was added and the alcoholic solvent was removed under reduced pressure. This aqueous mixture was then extracted twice with dichloromethane. The combined organic extracts were washed with water and brine, dried over sodium sulfate, and concentrated. The crude mixture was purified by flash chromatography to afford the title compound.^{25–27}

4.4.5. General procedure for conversion of 2*H*-indazoles into 1*H*-indazolones (5a–5f)

The precursor 2*H*-indazole (0.813 mmol) was dissolved in MeOH (4 mL) in a sealed microwave vial. H₂SO₄ (4.07 mmol) was added and heated at 100 °C overnight. This solution was then allowed to room temperature and neutralized with a saturated solution of NaHCO₃. This aqueous solution was extracted with EtOAc (3 × 25 mL) and the combined organic extracts were dried over anhydrous sodium sulfate and concentrated. This crude material was then purified by flash chromatography to afford the title compound.²⁸

4.4.6. General procedure for the synthesis of N¹,N²-disubstituted-1*H*-indazolones (6a–6f)

The requisite indazole (205 mg, 1.08 mmol) was added to a two-neck round bottom flask fitted with a water-cooled reflux condenser and an N₂ balloon, then dissolved in dry acetonitrile (10 mL). R³X (334 μL, 4.32 mmol) was added and the solution was heated at reflux until TLC analysis showed consumption of the indazole. The acetonitrile was then removed under reduced pressure and the crude material was dissolved in ethyl acetate (30 mL). This solution was then poured into saturated sodium carbonate (20 mL) and the layers were separated. The organic extracts were then washed with water, brine, dried over sodium sulfate, and concentrated. This crude material was purified by flash chromatography to afford the title compound.²⁹

4.4.7. General procedure for the synthesis of thiazolo- and thiazolino-2*H*-indazoles (12a–12d)

2-Nitrobenzaldehyde or 6-nitropiperonal (1.1 equiv) and requisite 5-trityl protected 1°-aminothioalkanes (1 equiv) were dissolved in MeOH (0.4 M) in a 50 mL round-bottomed flask. The solution was stirred until TLC showed consumption of the starting 1°-aminothioalkanes. Sodium cyanoborohydride (2 equiv) was added portionwise and this solution was stirred until TLC showed consumption of imine. The solution was concentrated and the resulting residue was redissolved in methylene chloride. The organic layer was washed twice with 1 M HCl, dried over sodium sulfate and concentrated to ~15 mL. To this solution was added an equal volume of TFA, followed by triethylsilane (3 equiv). The solution was stirred for 30 min then concentrated. KOH (15 equiv), MeOH (0.1 M) and 10% H₂O were added to the flask and the solution was heated in a 90 °C oil bath for 3–6 h. Upon reaction completion, the MeOH was evaporated and the remaining aqueous solution was partitioned with EtOAc. The aqueous layer was

extracted twice with EtOAc and then the organic extracts were combined, washed with brine, dried over Na₂SO₄, and concentrated. Purification by silica gel chromatography provided products **12a–12d**.³⁰

Acknowledgments

We thank the *Tara K. Telford Fund for Cystic Fibrosis Research at the University of California-Davis* and the National Institutes of Health – United States (Grants HL092506, DK72517 and GM089153) for generous financial support of this work and gratefully acknowledge OpenEye for providing software. A.R. and S.O. contributed equally to this work.

Supplementary data

Supplementary data (docking images, ¹H and ¹³C NMR spectra, and full experimental protocols) associated with this article can be found, in the online version, at <http://dx.doi.org/10.1016/j.bmc.2014.09.044>.

References and notes

1. Arnold, J.; Flemmig, J. *Arch. Biochem. Biophys.* **2010**, *500*, 92.
2. Klebanoff, S. J. *J. Leukocyte Biol.* **2005**, *77*, 598.
3. Metzler, K. D.; Fuchs, T. A.; Nauseef, W. M.; Reumaux, D.; Roesler, J.; Schulze, I.; Wahn, V.; Papayannopoulos, V.; Zychlinsky, A. *Blood* **2011**, *117*, 953.
4. Prokopowicz, Z.; Marcinkiewicz, J.; Katz, D. R.; Chain, B. M. *Arch. Immunol. Ther. Exp. (Warsz)* **2012**, *60*, 43.
5. van der Veen, B. S.; de Winther, M. P. J.; Heeringa, P. *Antioxid. Redox Signal.* **2009**, *11*, 2899.
6. Rowe, S. M.; Miller, S.; Sorscher, E. J. *N. Eng. J. Med.* **2005**, *352*, 1992.
7. Garner, H. P.; Phillips, J. R.; Herron, J. G.; Severson, S. J.; Milla, C. E.; Regelman, W. E. *J. Lab. Clin. Med.* **2004**, *144*, 127.
8. Thompson, E.; Brennan, S.; Senthilmohan, R.; Gangell, C. L.; Chapman, A. L.; Sly, P. D.; Kettle, A. J. *Free Radical Biol. Med.* **2010**, *49*, 1354.
9. Van Der Vliet, A.; Nguyen, M. N.; Shigenaga, M. K.; Eiserich, J. P.; Marelich, G. P.; Cross, C. E. *Am. J. Physiol. Lung Cell* **2000**, *279*, 537.
10. Regelman, W. E.; Siefferman, C. M.; Herron, J. G.; Elliott, G. R.; Clawson, C. C.; Gray, B. H. *Pediatr. Pulmonol.* **1996**, *19*, 1.
11. Van Der Vliet, A.; Eiserich, J. P.; Marelich, G. P.; Halliwell, B.; Cross, C. E. *Adv. Pharmacol.* **1997**, *38*, 491.
12. Nussbaum, C.; Klinke, A.; Adam, M.; Baldus, S.; Sperandio, M. *Antioxid. Redox Signal.* **2013**, *18*, 692.
13. Cantin, A. M.; White, T. B.; Cross, C. E.; Forman, H. J.; Sokol, R. J.; Borowitz, D. *Free Radical Biol. Med.* **2007**, *42*, 15.
14. Kettle, A. J.; Chan, T.; Osberg, I.; Senthilmohan, R.; Chapman, A. L.; Mocatta, T. J.; Wagener, J. S. *Am. J. Respir. Crit. Care Med.* **2004**, *170*, 1317.
15. Gorudko, I. V.; Grigorieva, D. V.; Shamova, E. V.; Kostevich, V. A.; Sokolov, A. V.; Mikhailchik, E. V.; Cherenkevich, S. N.; Arnold, J.; Panasenko, O. M. *Free Radical Biol. Med.* **2014**, *68*, 326.
16. Huang, Y.; DiDonato, J. A.; Levison, B. S.; Schmitt, D.; Li, L.; Wu, Y.; Buffa, J.; Kim, T.; Gerstenecker, G. S.; Gu, X.; Kadiyala, C. S.; Wang, Z.; Culley, M. K.; Hazen, J. E.; DiDonato, A. J.; Fu, X.; Berisha, S. Z.; Peng, D.; Nguyen, T. T.; Liang, S.; Chuang, C.-C.; Cho, L.; Plow, E. F.; Fox, P. L.; Gogonea, V.; Tang, W. H. W.; Parks, J. S.; Fisher, E. A.; Smith, J. D.; Hazen, S. L. *Nat. Med.* **2013**, *20*, 193.
17. Reynolds, W.F.; Sermet-Gaudelus, I.; Gausson, V.; Feuillet, M.-N.; Bonnefont, J.P.; Lenoir, G.; Descamps-Latscha, B.; Wikko-Sarsat, V. *Mediat. Inflamm.* **2006**, <http://dx.doi.org/10.1155/mi/2006/36735>.
18. Malle, E.; Furtmuller, P. G.; Sattler, W.; Obinger, C. *Br. J. Pharmacol.* **2007**, *152*, 838.
19. Chung, A.; Marshall, C. V.; Sin, D. D.; Bolton, S.; Zhou, S.; Thain, K.; Cadogan, E. B.; Maltby, J.; Soars, M. G.; Mallinder, P. R.; Wright, J. L. *Am. J. Respir. Crit. Care Med.* **2012**, *185*, 34.
20. Forbes, L. V.; Sjogren, T.; Auchere, F.; Jenkins, D. W.; Thong, B.; Laughton, D.; Hemsley, P.; Pairedeau, G.; Turner, R.; Eriksson, H.; Unitt, J. F.; Kettle, A. J. *J. Biol. Chem.* **2013**, *51*, 36636.
21. Tidén, A. K.; Sjogren, T.; Svensson, M.; Bernlind, A.; Senthilmohan, R.; Auchère, F.; Norman, H.; Markgren, P. O.; Gustavsson, S.; Schmidt, S.; Lundquist, S.; Forbes, L. V.; Magon, N. J.; Paton, L. N.; Jameson, G. N.; Eriksson, H.; Kettle, A. J. *J. Biol. Chem.* **2011**, *43*, 37578.
22. Soubhye, J.; Prevost, M.; Van Antwerpen, P.; Zouaoui Boudjeltia, K.; Rousseau, A.; Furtmuller, P. G.; Obinger, C.; Vanhaeverbeek, M.; Ducobu, J.; Neve, J.; Gelbcke, M.; Dufresne, F. O. *J. Med. Chem.* **2010**, *53*, 8747.
23. Mills, A. D.; Nazer, M. Z.; Haddadin, M. J.; Kurth, M. J. *J. Org. Chem.* **2006**, *71*, 2687.
24. Oakdale, J. S.; Solano, D. M.; Fettingter, J. C.; Haddadin, M. J.; Kurth, M. J. *Org. Lett.* **2009**, *11*, 2760.

25. Butler, J. D.; Solano, D. M.; Robins, L. I.; Haddadin, M. J.; Kurth, M. J. *J. Org. Chem.* **2008**, *73*, 234.
26. Donald, M. B.; Conrad, W. E.; Oakdale, J. S.; Butler, J. D.; Haddadin, M. J.; Kurth, M. J. *Org. Lett.* **2010**, *12*, 2524.
27. Avila, B.; Solano, D. M.; Haddadin, M. J.; Kurth, M. J. *Org. Lett.* **2011**, *13*, 1060.
28. Conrad, W. E.; Fukazawa, R.; Haddadin, M. J.; Kurth, M. J. *Org. Lett.* **2011**, *13*, 3138.
29. Conrad, W. E.; Rodriguez, K. X.; Nguyen, H. H.; Fettingner, J. C.; Haddadin, M. J.; Kurth, M. J. *Org. Lett.* **2012**, *14*, 3870.
30. Farber, K. M.; Haddadin, M. J.; Kurth, M. J. *J. Org. Chem.* **2014**, *79*, 6939.
31. Hawkins, P. C. D.; Skillman, A. G.; Warren, G. L.; Ellingson, B. A.; Stahl, M. T. *J. Chem. Inf. Model.* **2010**, *50*, 572.
32. *OpenEye Scientific Software, I, version 1.7.4 ed.*; OpenEye: Santa Fe, NM, 2010. <http://www.eyesopen.com>.
33. Hawkins, P. C. D.; Nicholls, A. J. *J. Chem. Inf. Model.* **2012**, *52*, 2919.
34. Soubhye, J.; Aldib, I.; Elfving, B.; Gelbcke, M.; Furtmüller, P. G.; Podrecca, M.; Conotte, R.; Colet, J.-M.; Rousseau, A.; Reye, F.; Sarakbi, A.; Vanhaeverbeek, M.; Kauffmann, J.-M.; Obinger, C.; Nève, J.; Prévost, M.; Zouaoui Boudjeltia, K.; Dufresne, F.; Van Antwerpen, P. *J. Med. Chem.* **2013**, *56*, 3943.
35. Sliskovic, I.; Abdulhamid, I.; Sharma, M.; Abu-Soud, H. M. *Free Radical Biol. Med.* **2009**, *47*, 1005.
36. Van Antwerpen, P.; Prévost, M.; Zouaoui-Boudjeltia, K.; Babar, S.; Legssyer, I.; Moreau, P.; Mogueilevsky, N.; Vanhaeverbeek, M.; Ducobu, J.; Nève, J.; Dufresne, F. *Bioorg. Med. Chem.* **2008**, *16*, 1702.
37. Veber, D. F.; Johnson, S. R.; Cheng, H.; Smith, B. R.; Ward, K. W.; Kopple, K. D. *J. Med. Chem.* **2002**, *45*, 2615.
38. Hou, T. J.; Xu, X. *J. Chem. Inf. Comput. Sci.* **2003**, *43*, 2137.
39. Choi, D. K.; Pennathur, S.; Perier, C.; Tieu, K.; Teismann, P.; Wu, D. C.; Jackson-Lewis, V.; Vila, M.; Vonsattel, J.; Heinecke, J. W.; Przedborski, S. *J. Neurosci.* **2005**, *25*, 6594.
40. Kajer, T. B.; Fairfull-Smith, K. E.; Yamasaki, T.; Yamada, K.; Fu, S.; Bottle, S. E.; Hawkins, C. L.; Davies, M. J. *Free Radical Biol. Med.* **2014**, *70*, 96.
41. van der Does, A. M.; Hensbergen, P. J.; Bogaards, S. J.; Cansoy, M.; Deelder, A. M.; van Leeuwen, H. C.; Drijfhout, J. W.; van Dissel, J. T.; Nibbering, P. H. *J. Immunol.* **2012**, *10*, 5012.
42. Frisch, M. J. *Gaussian 09, Revision B.01*; Gaussian: Wallingford, CT, 2010 (for full reference, see Supporting information).
43. Dypbukt, J. M.; Bishop, C.; Brooks, W. M.; Thong, B.; Eriksson, H.; Kettle, A. J. *Free Radical Biol. Med.* **2005**, *39*, 1468.